Research paper

Kinetic study of marine and lacustrine shale grains using Rock-Eval pyrolysis: Implications to hydrocarbon generation, retention and expulsion

Lingling Liao [a], Yunpeng Wang [a, *], Chengsheng Chen [a, b], Shuyong Shi [a, b], Rui Deng [a, b]

[a] State Key Laboratory of Organic Geochemistry, Guangzhou Institute of Geochemistry, Chinese Academy of Sciences, Guangzhou 510640, China
[b] University of the Chinese Academy of Science, Beijing 100039, China

ARTICLE INFO

ABSTRACT

The kinetic parameters of marine and lacustrine shale grains (4 mm) were retrieved by using Rock-Eval pyrolysis in comparison with finely ground powder (<0.178 mm) and kerogen of same samples. Results of grains show remarkable differences from powder and kerogen. Grains of Pingliang marine shale exhibit a relatively broader distribution of activation energies than powder and kerogen while grains of Yanchang lacustrine shale show higher dominant activation energies than powder and kerogen. At laboratory heating rates (5–25 °C/min), the corresponding temperatures to the maximum hydrocarbon generating rate of grains are 3–8 °C higher than powder and kerogen for marine shale and 6–8 °C higher for lacustrine shale, respectively. Extrapolated to geological heating rate (3 °C/my), the corresponding maturity and geological temperature to the maximum hydrocarbon expulsion rate of grains lags powder 0.02 Ro% and 3 °C, as well as 0.05 Ro% and 6 °C for marine shale and lacustrine shale, respectively. After the peak of hydrocarbon generation (Ro = 1%), the retention percentage for grain and powder of marine shale reach 7.33% and 0.09% while those for lacustrine shale reach 16.50% and 10.85%, respectively. These results suggest grains enjoy higher expulsion threshold and higher retention ability. The results suggest that Yanchang lacustrine shale exhibits stronger retention ability and weaker expulsion ability than Pingliang marine shale. The results presented in this study show that grain-based pyrolysis provides a novel method for evaluating the residual oil and gases for shale, which can study the hydrocarbon generation, expulsion and retention comprehensively.

© 2017 Elsevier Ltd. All rights reserved.

1. Introduction

Recent studies and explorations have shown great potentials of unconventional oil gas resources such as shale gas and shale oil, which indicates an important role of retained hydrocarbons in source rocks(Jia et al., 2014). But till to now, we still lack effective method to evaluate retained hydrocarbons in source rocks. It is regarded that retained hydrocarbon should be evaluated together with hydrocarbon generation and expulsion. Traditional method usually evaluates hydrocarbon generation and expulsion separately. Rock-Eval, Micro-Scaled Sealed Vessel (MSSV) and gold-tube systems are widely used pyrolysis methods for retrieving kinetics of hydrocarbon generations. In most cases, geochemists are tending to use kerogen not rock itself for pyrolysis (Behar et al., 1992). However, these results are from the kerogen not its mother-rock, focusing on thermal degradation behavior of organic matter. Actually, hydrocarbon generation process can be reflected by kerogen-based kinetics while hydrocarbon expulsion process is not only related to kerogen degradation but also to the whole rock. Knowledge of retained hydrocarbon and its evolution in source rocks are also less studied (Dembicki, 1992).

Rock-Eval instrument was developed by Institution of French Petroleum in 1970s to perform anhydrous, open system pyrolysis (Espitalié et al., 1977), which is extensively used for source rock evaluation due to its rapid speed, simple operation and small requirement of samples. It produces reliable data by screening petroleum generative potential and thermal maturity (Sykes and Snowdon, 2002); Oil and gas formation from source rock is generally attributed to progressive catagenesis of kerogen and bitumen with increasing temperature and burial depth in

sedimentary basins (Tissot and Espitalie, 1975; Wei et al., 2012). The formation of oil and gas in nature is controlled by chemical reaction kinetics which can be modeled under laboratory conditions, and then the laboratory-derived kinetic parameters can be applied into geological setting to simulate the process of petroleum formation in sedimentary basins (İnan and Schenk, 2001).

In this paper, we attempt to evaluate hydrocarbon generation, retention and expulsion by using a grain-based Rock-Eval pyrolysis in comparing with powder and kerogen ones. The main reason is that the grain-based pyrolysis can simulate the process of hydrocarbon generation, retention and expulsion simultaneously. Three forms of samples including grain, powder and kerogen from one marine and one lacustrine shale were pyrolyzed using Rock-Eval system. Here, grain represents natural state integrating hydrocarbon generation, retention and expulsion, isolated kerogen represents hydrocarbon generation of pure organic matters, and powder represents the mixture of mineral matrix and organic matter. The kinetic parameters of grain, powder and kerogen were retrieved by using Kinetics 2000 software, which were used to extrapolate the laboratory results to geological conditions.

2. Samples and experiments

2.1. Samples

For better understanding the whole process of hydrocarbon generation, retention and expulsion of marine and lacustrine shale, two low maturated rock samples representing different lithological depositions were selected. One is marine shale from an outcrop of middle Ordovician Pingliang formation (PL-M, O_2p) and the other is lacustrine shale from a borehole (Well Zheng8) of Upper Triassic Yanchang formation (YC-L, T_3y). Both samples are from Erdos Basin (China) and their geochemical data listed in Table 1. Two samples show higher TOC contents, typeⅡkerogen and lower maturities which are suitable for simulation. Grain and power from marine and lacustrine shale show slight difference in total organic carbon (TOC), respectively. The samples were prepared into three forms including grain (diameter in 4 mm), power (<0.178 mm) and kerogen, which were subjected to Rock-Eval programmed-temperature pyrolysis. To guaranty that samples in different heating rates are identical and the influence of sample heterogeneity is negligible, we took samples from one rock using micro-drilling method along vertical direction because the heterogeneity of shale rock is mainly along horizontal direction. Detailed information on the sample achieving was described in our previous paper (Liao et al., 2016).

2.2. Pyrolysis

The Rock-Eval pyrolysis method has been widely used for oil and gas exploration in sedimentary basins over the world. This technique uses temperature programmed heating of a small amount of rock or coal in an inert atmosphere (helium or nitrogen) in order to determine the quantity of free hydrocarbons present in the sample and of those that can be potentially released after pyrolysis (Behar et al., 2001). The sample of different forms was subjected to pyrolysis using a Rock-Eval 6 instrument, allowing the measurement of TOC content, free hydrocarbons (S_1), hydrocarbon generative potential (S_2), carbon dioxide (CO_2) content produced during thermal cracking (S_3), and temperature (Tmax) at the maximum of the S_2 peak.

Samples of three different forms were pyrolyzed at the heating rates of 5 °C/min, 15 °C/min and 25 °C/min, respectively. The pyrolysis experiment was performed in Rock-Eval6 instrument (Behar et al., 2001). Products released from the source rocks were detected by flame ionization detector (FID) and thermal conductivity detector (Lehne and Dieckmann, 2007). The pyrolysis temperatures are from 300 °C to 600 °C at different heating rates to characterize Tmax, S_1, S_2, S_3, and TOC contents, and then obtain the hydrocarbon yield through formula (S_2/TOC) (Langford and Blanc-Valleron, 1990; Schenk and Horsfield, 1993; Geng and Liao, 2002). For better comparison, samples in different forms were carried out in the same apparatus and experimental conditions. To make sure the reliability of the experiment, we carried out a parallel pyrolysis for grain, powder and kerogen samples of both marine and lacustrine shale. To avoid the differences caused by sample weights, we took the same weight of samples for grain and powder using an electronic scale with error range of ±0.05 mg. Before each pyrolysis experiment, a standard sample was tested to ensure the instrument normal. According our test, the error range of S_2, Tmax and TOC are 5%, ±2°Cand ±0.14%, respectively.

2.3. Kinetic modelling

The simulation are performed at higher temperature of laboratory conditions, and substantially the reactions are much more rapid than those occurring under geological conditions (Tissot et al., 1987; Ungerer and Pelet, 1987; Ungerer, 1990; Tang and Stauffer, 1994; Tang et al., 2000). In this study, Rock-Eval pyrolysis at multiple heating rates aim to derive kinetic parameters which can be applied into geothermal histories for studying the evolution process of oil and gas in sedimentary basin (Behar et al., 1997; İnan and Schenk, 2001; Han et al., 2014).

Kinetic modelling is considered as the mathematical links between fast laboratory reactions and slow reactions occurred under geological conditions. The kinetic models are based on the first order kinetic laws, in which the kerogen degradation can be approximately described by the Arrhenius equation (Tissot and Welte, 1984; Ungerer and Pelet, 1987; İnan and Schenk, 2001)

Table 1
Samples used in the pyrolysis study and their geochemical characteristics.

Sample	Location	Lithology	Forms	S_1 (mg/g)	S_2 (mg/g)	Tmax (°C)	TOC (%)	Ro (%)	Kerogen type
PL-M	Erdos Basin	Marine shale	Grain	2.39	74.57	433	19.49	0.60	II$_1$
			Powder	4.50	78.07	429	19.85		
			Kerogen	12.03	232.99	428	53.46		
YC-L	Erdos Basin	Lacustrine shale	Grain	3.93	55.45	442	21.87	0.64	II$_1$
			Powder	6.12	63.91	434	19.59		
			Kerogen	21.86	254.80	433	58.6		

TOC: Total Organic Carbon; S1: Free Hydrocarbons; S2: Pyrolysis of Hydrocarbons; Tmax: Pyrolysis Temperature at Maximum Hydrocarbon Generation; Ro: Vitrinite Reflectance (%).

$$dx_i/dt = -Ax_i \exp\left(-\frac{E_i}{RT}\right), i = 1...N \qquad (1)$$

Where x_i is the residual potential of petroleum formation associated to reaction i, t is time, T is temperature, R is molar gas constant, and A is frequency factor while E_i is the assumed activation energies (Braun and Burnham, 1990; Burnham and Braun, 1999; İnan and Schenk, 2001; Wei et al., 2012). Bulk kinetic parameters (activation energy E_i and frequency factor A) for kerogen to hydrocarbon conversion are calculated on the basis of the mathematical routine (Han et al., 2014). Assuming parallel first-order reactions with a single frequency factor and activation energies, different heating rates are used to achieve optimal values. Optimization results in a best fit for calculated curves and measured curves (Han et al., 2014). Calculating the experiment data of grain, powder and kerogen at different heating rates from marine shale (PL-M) and lacustrine shale (YC-L) by Kinetics 2000 software, while the activation energy obey the discrete distributed model (Miura, 1995).

The optimization performed within the Kinetics 2000 software developed by Lawrence Livermore National Laboratory (LLNL) and Humble Instruments & Services. Kinetic parameters consist of a discrete activation energy distribution with a single frequency factor. The use of a single frequency factor for all reactions was justified by the empirical need to reduce the number of unknown parameters, rather than theoretical considerations (Ungerer and Pelet, 1987; Ungerer, 1990; Abbassi et al., 2016). The discrete model was detailed description by (Burnham et al., 1987).

3. Results and discussion

3.1. The influence of heating rate on hydrocarbon generation and expulsion

Fig. 1 and Fig. 2 show the hydrocarbon generation rates (mg/g.s^{-1}) and hydrocarbon yield of grain, powder and kerogen from Pingliang marine shale (PL-M) and Yanchang lacustrine shale (YC-L) as a function of pyrolysis temperature at different heating rates. The pyrolysis characteristics for grain, powder and kerogen from marine shale are similar to lacustrine shale. The faster the pyrolysis heating rates are, the faster the hydrocarbon generating rates are, which are similar for grain, powder and kerogen. The corresponding temperature to the maximum hydrocarbon generation rate increases with heating rates. The highest is found at the heating rate of 25 °C/min, followed by 15 °C/min and 5 °C/min. The cumulative yields of hydrocarbon yield increase with the increasing pyrolysis temperature for grain, powder and kerogen. The corresponding hydrocarbon yield at the same pyrolysis temperature for 5 °C/min heating rate is greater than those at 15 °C/min and 25 °C/min, and similarly the hydrocarbon yield for 15 °C/min is greater than that for 25 °C/min. The faster the pyrolysis heating rate is, the slighter the influence on the increasing of the hydrocarbon yield is. Similarly, the faster the pyrolysis heating rate is, the higher the corresponding temperature to the maximum hydrocarbon yield is. Whether at the fast or slow heating rates, the final production curves of hydrocarbon yield are coincided together, which indicates the pyrolysis heating rates does not affect the total amount of hydrocarbon generation of source rocks. The results clearly show grain and powder from marine shale (PL-M) and lacustrine shale (YC-L) exhibit similar pyrolysis characteristics with kerogen in both hydrocarbon generating rates and hydrocarbon yield at different heating rates. Because kerogen represents the typical pyrolysis regularity of organic matter (Behar et al., 1992), it means that the pyrolysis of grain and powder samples are dominantly showing the behavior of organic matter. So it is feasible to study the evolution of

hydrocarbon generation, expulsion and retention by using grain-based Rock-Eval pyrolysis experiments.

3.2. The influence of sample forms on hydrocarbon expulsion

Fig. 3 shows that marine shale (PL-M) and lacustrine shale (YC-L) have a good consistency in hydrocarbon generating rates at different heating rates for grain, powder and kerogen, respectively. Corresponding to the maximum hydrocarbon generating rate, grain shows the highest pyrolysis temperature among the three sample forms, while powder shows similar temperatures with kerogen. For the grain of marine shale (PL-M), the corresponding pyrolysis temperatures to the maximum hydrocarbon generating rates are 3 °C, 8 °C and 7 °C higher than those of powder and kerogen at the heating rates of 5 °C/min, 15 °C/min and 25 °C/min, respectively. For the grain of lacustrine shale (YC-L), the corresponding pyrolysis temperatures to the maximum hydrocarbon generating rates are 6 °C, 8°Cand 8 °C higher than those of powder and kerogen at the heating rates of 5 °C/min, 15 °C/min and 25 °C/min, respectively. The grain-based pyrolysis show somehow lagging effects and the reason might be that the products of rock grain include both generation and expulsion processes, which leads to the generated hydrocarbon cannot be expelled out in time (Inan et al., 1998).

Fig. 4 shows grain, powder and kerogen from marine shale (PL-M) and lacustrine shale (YC-L) overlap in low pyrolysis temperature (300–400 °C). With increasing of pyrolysis temperature, grain for marine shale (PL-M) and lacustrine shale (YC-L) show significantly difference from powder and kerogen in hydrocarbon yield. The main reason is that hydrocarbon expulsion is relatively difficult to occur in low temperature. For both marine shale (PL-M) and lacustrine shale (YC-L), grain and powder show lower hydrocarbon yield than kerogen at all heating rates. With the increasing of pyrolysis temperature, the difference of hydrocarbon yield of grain and powder from kerogen for lacustrine shale (YC-L) is more obvious than marine shale (PL-M) at all heating rates. Take 15 °C/min for example, the difference of hydrocarbon yield for marine shale (PL-M) is around 35 mg/g TOC between grain and kerogen, and around 15 mg/g TOC between powder and kerogen at 600 °C, while those for lacustrine shale (YC-L) are around 71 mg/g TOC and 60 mg/g TOC, respectively. The results indicate that some of generated hydrocarbon might be retained in grain and powder due to its retention and adsorption capabilities. In comparison, lacustrine shale (YC-L) shows stronger retention capability than marine shale (PL-M).

3.3. Kinetic parameters

Kinetic parameters include activation energy and frequency factor computed by Kinetic 2000 software (Menzinger and Wolfgang, 1969; Behar et al., 1997; Wang et al., 2006; Han et al., 2014). Fig. 5 and Table 2 show the activation energy distribution as well as the frequency factor (A) for grain, powder and kerogen from marine shale (PL-M) and lacustrine shale (YC-L), respectively. For marine shale (PL-M), the discrete activation energy distributions range from 37 to 59, 36–59 and 36–59 kcal/mol with a universal frequency factor A = 4.15*10^{11}s^{-1} for grain, powder and kerogen, respectively. Clearly, grain, powder and kerogen exhibit the same dominant activation energy of 46 kcal/mol, which account for 74%, 48% and 50% of the kerogen conversion, respectively. The kinetic parameters of the grain display a relatively narrow distribution of activation energies, implying that grain enjoys a faster and later expulsion peak than powder and kerogen. For lacustrine shale (YC-L), the discrete activation energy distributions display the same range (38–61 kcal/mol) for grain, powder and kerogen with a common frequency factor A = 1.9829*10^{12}s^{-1}. Dominant activation
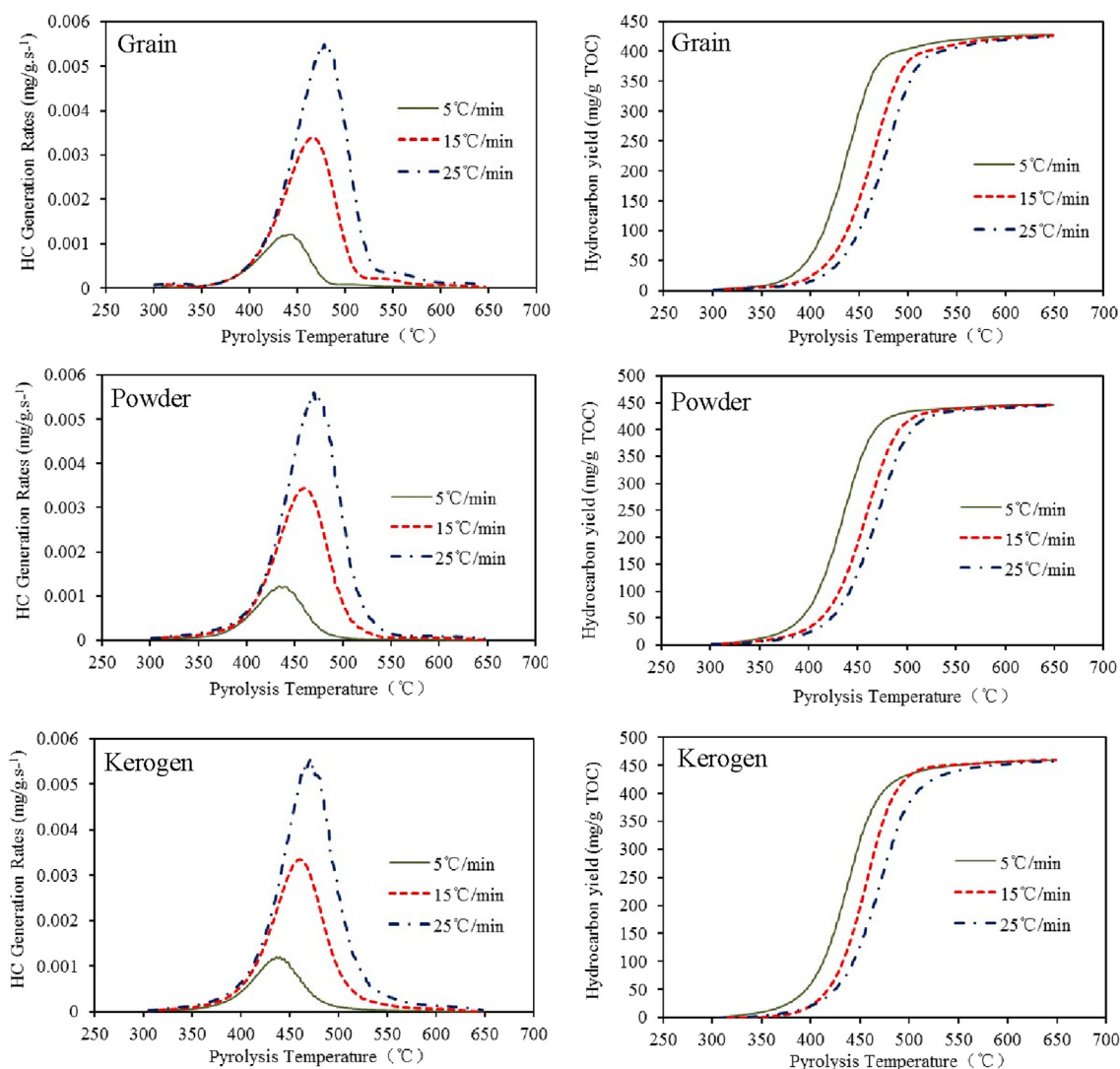
Fig. 1. Hydrocarbon (HC) generating rates and hydrocarbon yield of grain, powder and kerogen from Pingliang marine shale (PL-M) against pyrolysis temperatures at different heating rates.

energy for grain, powder and kerogen of YC-L shale are 49, 48 and 48 kcal/mol, respectively which account for 47%, 84% and 68% of kerogen conversion, respectively. YC-L grain exhibits a relatively higher dominant activation energy suggesting its higher expulsion threshold than powder and kerogen.

The results suggest grain is more difficult to expel hydrocarbon than powder for both marine shale (PL-M) and lacustrine shale (YC-L). Compared to marine shale (PL-M) and lacustrine shale (YC-L), lacustrine shale (YC-L) shows higher activation energy in grain, powder, and kerogen, which indicate lacustrine shale (YC-L) needs more energy to occur hydrocarbon expulsion.

3.4. Geological implications

For studying the characteristics of hydrocarbon generation, retention and expulsion, the laboratory results are extrapolated to geological heating rate of 3 °C/my (million years) using kinetic parameters, which is closed to the average geological heating rate in Erdos Basin (Schenk et al., 1997). Fig. 6 and Table 3 show a comparison of the conversion rate versus geological temperature and maturity (Ro%) for grain, powder and kerogen for marine shale (PL-M) and lacustrine shale (YC-L). The division of the main

hydrocarbon generation period (MHGP) according to the conversion rate between 10% and 90% (Pepper and Corvi, 1995) which account for the 80% of the total hydrocarbon generation in a certain stage of thermal evolution. For marine shale (PL-M), the corresponding maturity (Ro%) and geological temperature to MHGP for grain, powder and kerogen are 0.61–0.87% (108–141 °C), 0.58–0.78% (106–133 °C) and 0.58–0.85% (106–140 °C), respectively. For lacustrine shale (YC-L), the corresponding maturity (Ro%) and geological temperature to MHGP for grain, powder and kerogen are 0.65–0.99% (114–150 °C), 0.65–0.88% (114–142 °C) and 0.65–0.97% (114–149 °C), respectively. The results show grain exhibits a broader maturity and geological temperature than those of powder and kerogen for both marine shale (PL-M) and lacustrine shale (YC-L), which suggests that the MHGP of grain is relatively later due to expulsion. In comparison, grain and powder from lacustrine shale (YC-L) show broader range of maturity (Ro%) and geological temperature which indicates lacustrine shale is relatively difficult for hydrocarbon expulsion than marine shale (PL-M).

Fig. 7 shows the hydrocarbon expulsion rates for grain and powder of marine shale (PL-M) and lacustrine shale (YC-L) at a geological heating rate of 3 °C/my. For comparison, the hydrocarbon generation rates of kerogen from both marine and lacustrine
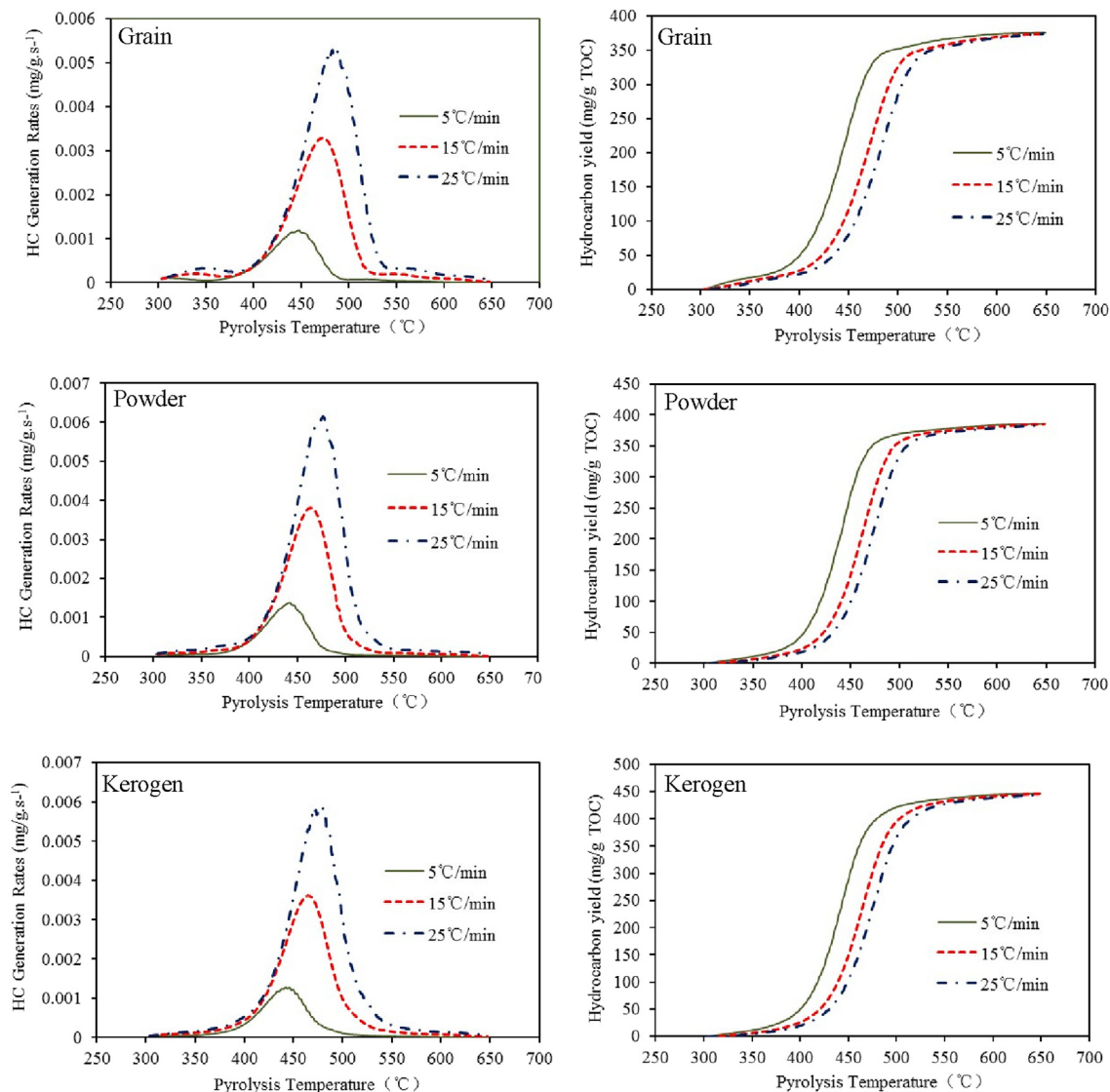
Fig. 2. Hydrocarbon (HC) generating rates and hydrocarbon yield of grain, powder and kerogen from Yanchang lacustrine shale (YC-L) against pyrolysis temperatures at different heating rates.

shale are also shown in Fig. 7. With increasing of temperature, there is an obvious hydrocarbon expulsion peak for grain and powder of marine shale (PL-M) and lacustrine shale (YC-L), respectively. After the maximum hydrocarbon expulsion peak, the expulsion rates decrease rapidly. For marine shale (PL-M), the corresponding Ro (%) and geological temperature to the maximum hydrocarbon expulsion rate for grain and powder are 0.72% (124 °C) and 0.70% (121 °C), respectively while those for lacustrine shale (YC-L) are 0.81% (136 °C) and 0.76% (130 °C), respectively. It is found that the corresponding Ro (%) and geological temperature to the maximum hydrocarbon expulsion rate for powder are identical with kerogen, which means that power-based pyrolysis results exhibit little information on hydrocarbon expulsion. In comparison to powder, the corresponding Ro% and geological temperature to the maximum hydrocarbon expulsion rate of grain lag 0.02 Ro%, 3 °C for marine shale (PL-M) and 0.05 Ro%, 6°Cfor lacustrine shale (YC-L), respectively. The reason lies in the fact that grain imposes some restriction on the flowing of generated hydrocarbons that makes the generated hydrocarbon cannot be expelled out in time (Inan et al., 1998; Inan, 2000). Interestingly, two shale samples in this study exhibit

different hydrocarbon expulsion ability. It seems the marine shale (PL-M) is easier to expel hydrocarbons. The corresponding Ro% and geological temperature to the maximum hydrocarbon expulsion rate of grain from marine shale (PL-M) are 0.09 Ro% (12 °C) earlier than those of lacustrine shale (YC-L). For powder, the results are similar, which are around 0.06 Ro% (9 °C) earlier than lacustrine shale (YC-L). This may be caused by the nature of source rock and the swelling capacity of kerogen (Inan et al., 1998; Wei et al., 2012). As further increasing of temperature, the hydrocarbon expulsion rates accelerate that makes the generated hydrocarbon partially expelled, forming a small and lower peak than the first one (Blanc and Connan, 1992).

Fig. 8 and Table 4 show the evolution of hydrocarbon generation, expulsion and retention for marine shale (PL-M) and lacustrine shale (YC-L) at a geological heating rates 3 °C/my. Here, two stages are selected for discussing: one is after the peak of hydrocarbon generation (Stage I: Ro = 1%) and the other is after second cracking (StageII: Ro = 3%). The Hydrocarbon yield of kerogen is assumed to represent the total hydrocarbon generation contents of organic matter, while Hydrocarbon yield of grain and powder
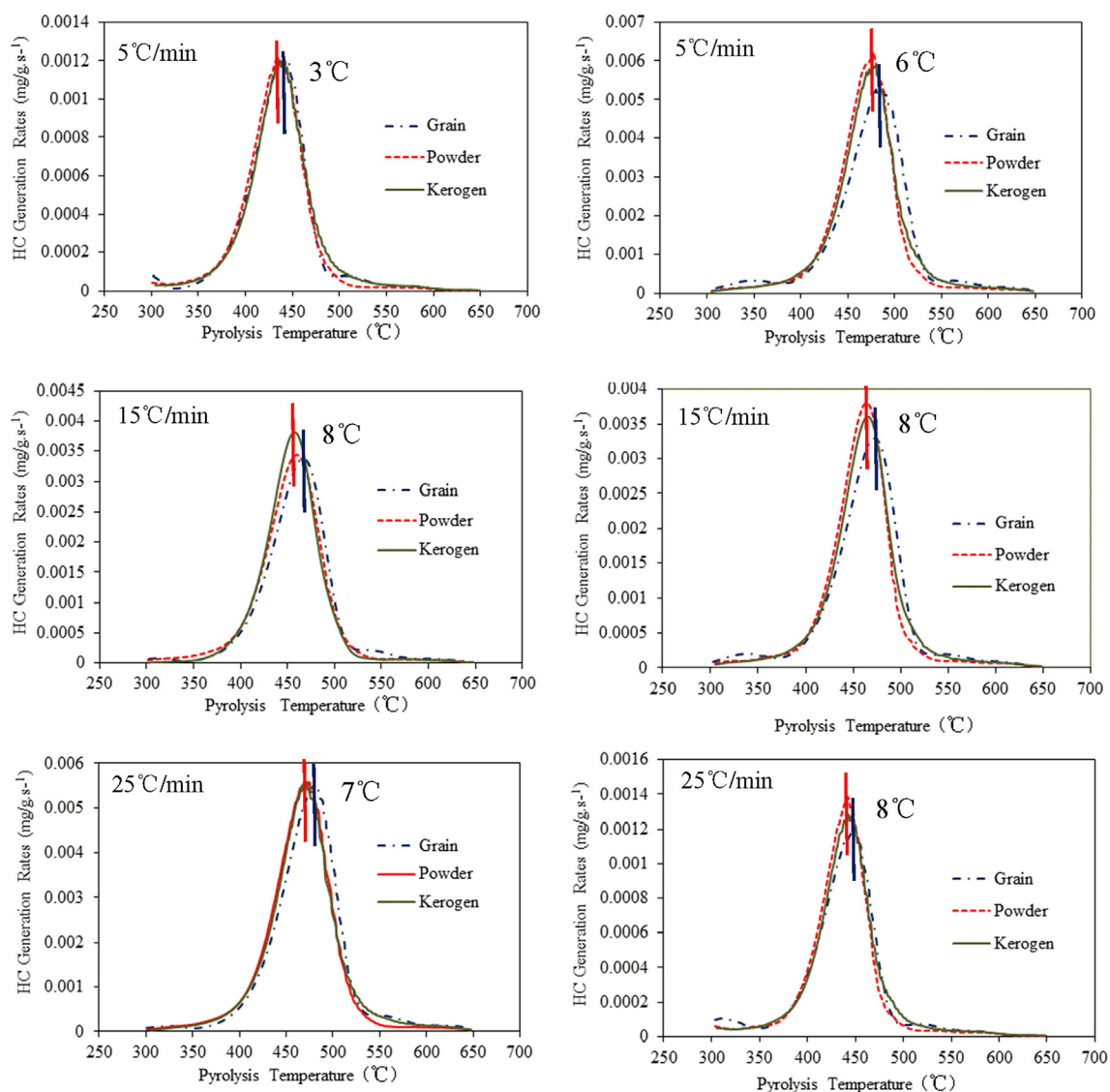
Fig. 3. Effects of different sample forms on hydrocarbon (HC) generating rate for Pingliang marine shale (left) and Yanchang lacustrine shale (right) at the heating rates of 5 °C/min, 15 °C/min and 25 °C/min.

represent the contents of hydrocarbon expulsion. So the retention for grain and powder are equivalent to hydrocarbon generation of kerogen minus the contents of hydrocarbon expulsion for grain and powder (Cornford et al., 1998). At stage I(Ro = 1%), the Hydrocarbon yield for grain, powder and kerogen for marine shale (PL-M) are 401.75 mg/g TOC, 433.16 mg/g TOC and 433.57 mg/g TOC, respectively while those for lacustrine shale (YC-L) are 338.59 mg/g TOC, 361.53 mg/g TOC and 405.51 mg/g TOC, respectively. The contents of hydrocarbon retention for grain and powder of marine shale (PL-M) are 31.82 mg/g TOC and 0.41 mg/g TOC while those for lacustrine shale (YC-L) are 66.92 mg/g TOC and 43.98 mg/g TOC, respectively. The retention percentages for grain and powder of marine shale (PL-M) are 7.33% and 0.09%, respectively while those for lacustrine shale (YC-L) are 16.50% and 10.85%, respectively. At stageII(Ro = 3%), the hydrocarbon yield for grain, powder, and kerogen of marine shale (PL-M) are 427.37 mg/g TOC, 446.53 mg/g TOC and 459.63 mg/g TOC, respectively while those for lacustrine shale (YC-L) are 375.09 mg/g TOC, 385.24 mg/g TOC and 445.75 mg/g TOC, respectively. The contents of hydrocarbon retention for grain and powder from marine shale (PL-M) are 32.26 mg/g TOC and

13.10 mg/g TOC while those for lacustrine shale (YC-L) are 70.66 mg/g TOC and 60.54 mg/g TOC, respectively. The retention percentages for grain and powder from marine shale (PL-M) are 7.02% and 2.85%, respectively while those for lacustrine shale (YC-L) are 15.85% and 13.58%, respectively. The total of hydrocarbon expulsion of grain is lower than powder for both marine shale (PL-M) and lacustrine shale (YC-L) which means that some of the generated hydrocarbon is retained in source rocks. The results suggest that grain-based pyrolysis is more likely to reflect both generation and expulsion process. According to the above results, the expulsion/retention capability of two samples in this study can be evaluated. Considering the hydrocarbon generation potentials (i.e. Hydrocarbon yield from kerogen) of marine shale (PL-M) and lacustrine shale (YC-L) are quite similar, the differences of grain-based results are more likely caused by expulsion/retention capability of the rock itself. The contents of hydrocarbon retention for lacustrine shale (YC-L) of grain and powder are much higher than those of marine shale (PL-M), which indicates that lacustrine shale (YC-L) enjoys higher ability to retain hydrocarbon.

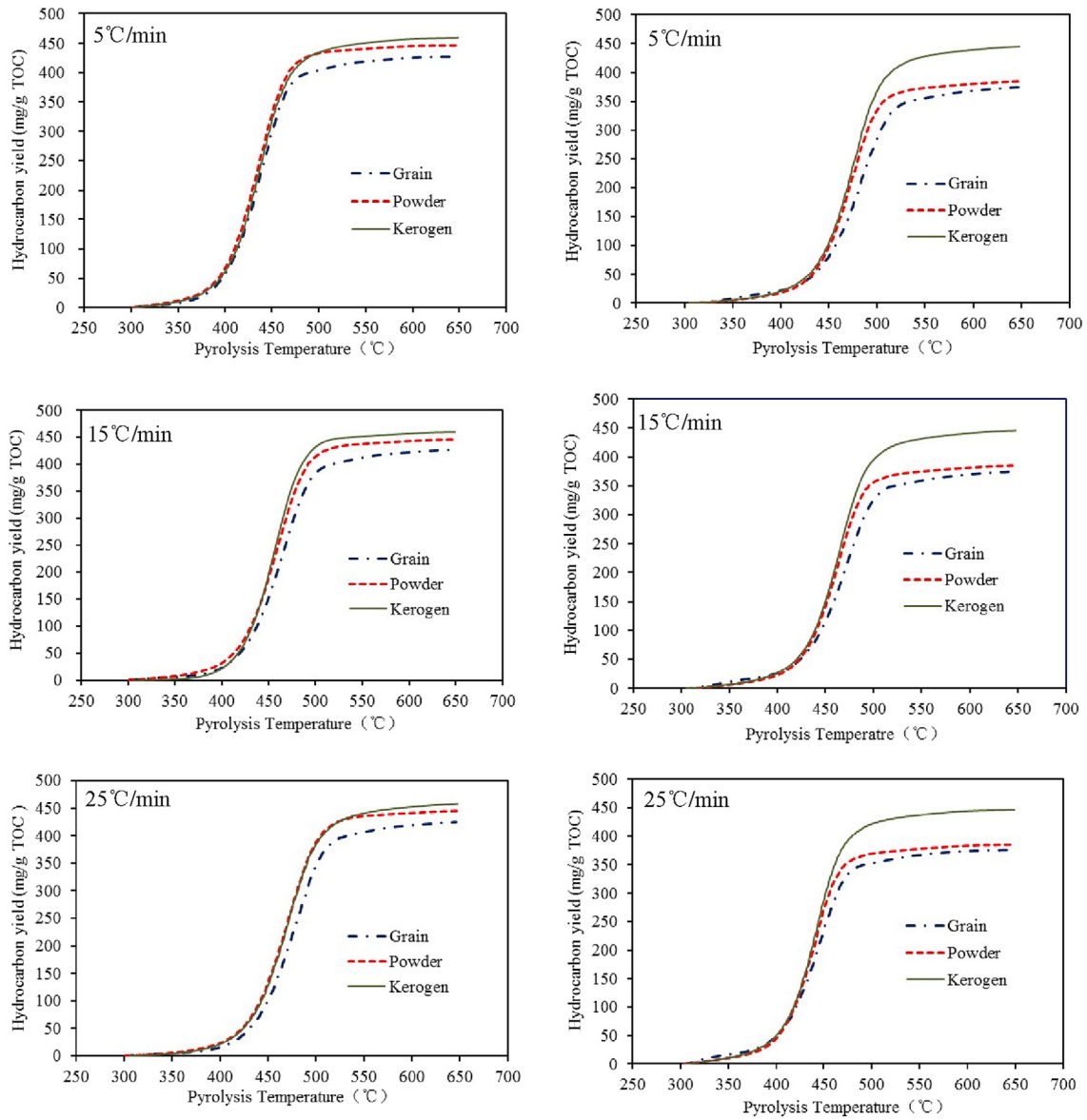One important issue is that the Yanchang lacustrine shale and

Fig. 4. Effects of different sample forms on hydrocarbon yield for Pingliang marine shale (left) and Yanchang lacustrine shale (right) at the heating rates of 5 °C/min, 15 °C/min and 25 °C/min.
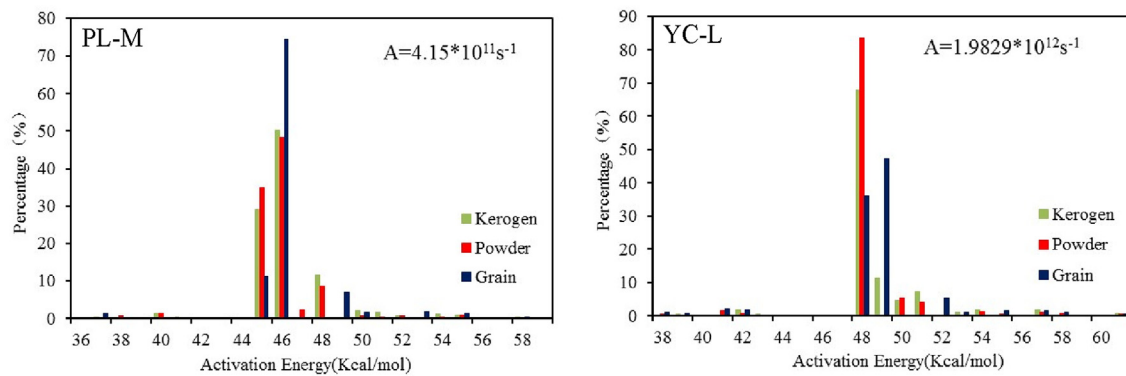

Fig. 5. Distribution of activation energies with universal frequency factor (A) for grain, powder and kerogen from marine shale (PL-M) and lacustrine shale (YC-L), respectively.

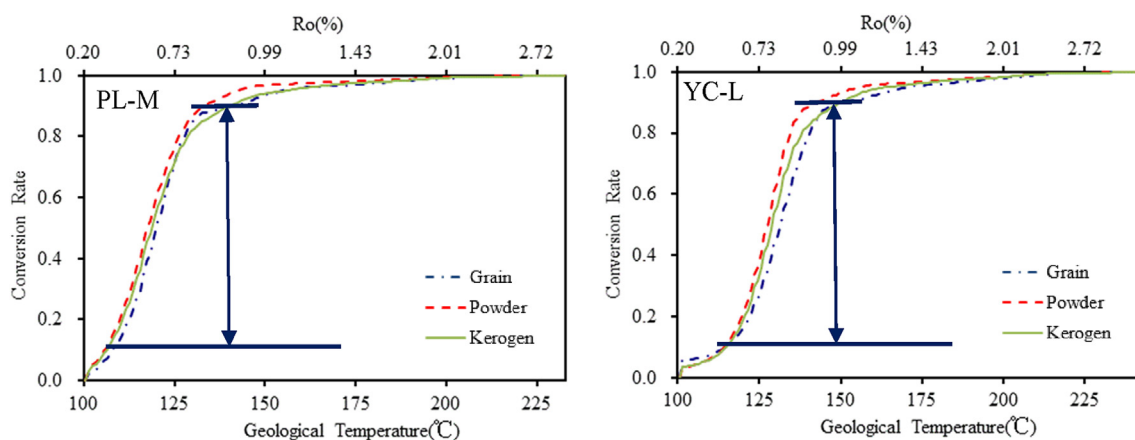Pingliang marine shale show great difference in retention ability. How to understand the phenomenon and what are main reasons are key and necessary to evaluate the method proposed in this study. According to the previous study, the mineral compositions of

Table 2
Kinetic parameters obtained from Rock-Eval pyrolysis for grain, powder and kerogen from marine shale (PL-M) and lacustrine shale (YC-L).

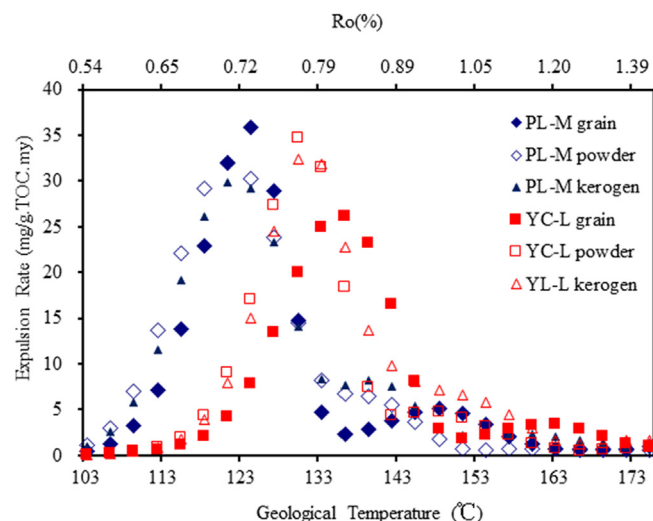| Sample	Forms	Ea range (Kcal/mol)	Emax (Kcal/mol)	$A(s^{-1})$
Pingliang marine shale	Grain	37–59	46	$A = 4.15*10^{11}s^{-1}$
	Powder	36–59	46	
	Kerogen	36–59	46	
Yanchang lacustrine shale	Grain	38–61	49	$A = 1.9829*10^{12}s^{-1}$
	Powder	38–61	48	
	Kerogen	38–61	48	

A is frequency factor; Ea is activation energy; Emax is the activation energy for maximum petroleum potential.

Fig. 6. The conversion rate versus geological temperature and maturity of Pingliang marine shale (PL-M) and Yanchang lacustrine shale (YC-L) at a geological heating rate of 3 °C/my.

Table 3
Division of main hydrocarbon generation period of Pingliang marine shale (PL-M) and Yanchang lacustrine shale (YC-L).

Sample	Forms	Main hydrocarbon generation period	
		Ro(%)	T(°C)
Pingliang marine shale	Grain	0.61–0.87	108–141
	Powder	0.58–0.78	106–133
	Kerogen	0.58–0.85	106–140
Yanchang lacustrine shale	Grain	0.65–0.99	114–150
	Powder	0.65–0.88	114–142
	Kerogen	0.65–0.97	114–149

Fig. 7. Expulsion rates of grain and powder for Pingliang marine shale (PL-M) and Yanchang lacustrine shale (YC-L) at geological heating rates of 3 °C/my.

the Yanchang shale and Pingliang shale are generally similar, which might have great influence on the retention ability of lacustrine and marine shale. However, the petro-physical properties of two suits of shale show obvious differences. Yanchang lacustrine shale is a kind of ultra-low permeability and low porosity shale (Zeng et al., 2008). The porosity of Yanchang shale ranges from 0.5 to 3.5%, and about 70% samples of Yanchange shale enjoy the permeability less than 0.01×10^{-3} μm^2. The pore diameter typically ranges from 6 to 9 nm with an average of 7.2 nm (Gao et al., 2014; Dai et al., 2016) while Pingliang marine shale show relatively higher porosity averagely between 4% and 6% and higher permeability averagely between 0.1×10^{-3} μm^2 and 2.0×10^{-3} μm^2 (Xu et al., 2013). Liu et al. (2015) studied the total pore volume and specific surface area for the marine shale and Chang-7 of Yanchang Formation shale. Their results also show that the total pore volume of Yanchang lacustrine shale is in the range of 0.001215–0.007495 cm^3/g and the specific surface area is between 0.38 and 3.03 m^2/g. The total pore volume and specific surface area of shale investigated are much less than those of the marine shale,

which may be attributed to the development degree of different types of pore in shale (Liu et al., 2015). These results suggest that the unique pore structures with low porosity and low permeability of Yanchang shale might be an important reason for its strong retention ability.

Experimental results also show sample forms affect the hydrocarbon expulsion. Grain and powder show similar characteristics of hydrocarbon generation with kerogen, which indicates that either grain or powder pyrolysis can still reflect the thermal degradation behavior of the organic matter in source rocks. However, there are
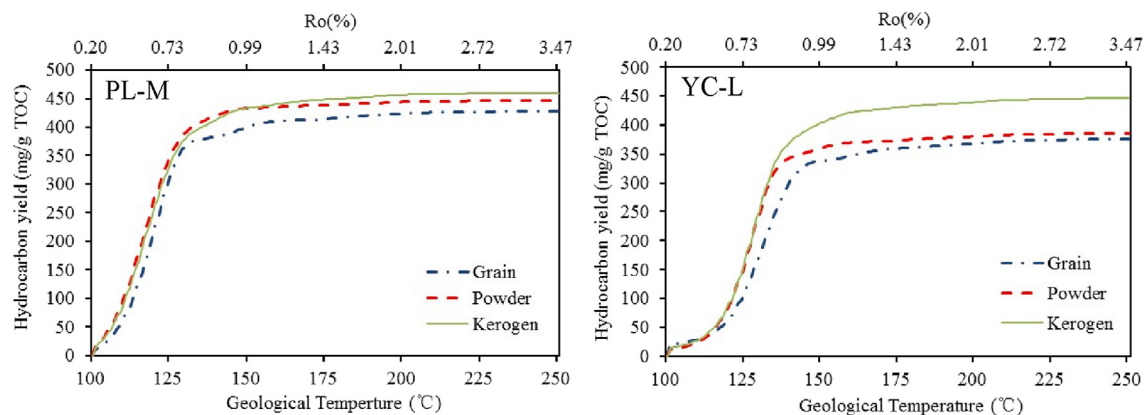
Fig. 8. Characteristics of hydrocarbon generation, retention and expulsion for grain, powder and kerogen from PL-M (left) and YC-L (right) at a geological heating rates of 3 °C/my.

Table 4
The amount of hydrocarbon generation, retention and expulsion for grain and powder from Pingliang marine shale (PL-M) and Yanchang lacustrine shale (YC-L) in StageI and StageII, respectively.

Sample	Forms	Ro = 1%			Ro = 3%		
		Hydrocarbon yield (mg/g TOC)	Retention (mg/g TOC)	Retention Percentage (%)	Hydrocarbon yield (mg/g TOC)	Retention (mg/g TOC)	Retention Percentage (%)
PL-M	Grain	401.75	31.82	7.33	427.37	32.26	7.02
	Powder	433.16	0.41	0.09	446.53	13.10	2.85
	Kerogen	433.57	–	–	459.63	–	–
YC-L	Grain	338.59	66.92	16.50	375.09	70.66	15.85
	Powder	361.53	43.98	10.85	385.24	60.54	13.58
	Kerogen	405.51	–	–	445.75	–	–

still some differences in Hydrocarbon yield, expulsion rate and corresponding temperatures both at laboratory conditions and natural conditions extrapolated using the kinetic parameters. Grain reflects not only the hydrocarbon generation but also the hydrocarbon expulsion of source rock. In contrast to grain, the main hydrocarbon generation periods (MHGP) of powder and kerogen are narrow which indicates that the hydrocarbon expulsions are rapid in geological conditions when the required expulsion threshold is met.

4. Conclusions

The kinetic parameters of grain, powder and kerogen from marine shale and lacustrine shale were obtained by Rock-Eval pyrolysis. For marine shale, the discrete activation energy distributions range from 37 to 59, 36 to 59 and 36 to 59 kcal/mol with a universal frequency factor $A = 4.15*10^{11}s^{-1}$ for grain, powder and kerogen, respectively. For lacustrine shale, the discrete activation energy distributions display the same range (38–61 kcal/mol) for grain, powder and kerogen with a universal frequency factor $A = 1.9829*10^{12}s^{-1}$.

The laboratory results are extrapolated to geological heating rate of 3 °C/my using kinetic parameters. For marine shale, the corresponding maturity and geological temperature to MHGP for grain, powder and kerogen are 0.61–0.87% (108–141 °C), 0.58–0.78% (106–133 °C) and 0.58–0.85% (106–140 °C), respectively. And for lacustrine shale (YC-L), the corresponding maturity (Ro%) and geological temperature to MHGP for grain, powder and kerogen are 0.65–0.99% (114–150 °C), 0.65–0.88% (114–142 °C) and 0.65–0.97% (114–149 °C), respectively.

For marine shale (PL-M), the corresponding Ro (%) and geological temperature to the maximum hydrocarbon expulsion rate for grain and powder are 0.72% (124 °C) and 0.70% (121 °C),

respectively while those for lacustrine shale (YC-L) are 0.81% (136 °C) and 0.76% (130 °C), respectively.

The results were also used to assess the hydrocarbon retention of source rocks. After the peak of hydrocarbon generation, the contents of hydrocarbon retention for grain and powder of marine shale are 31.82 mg/g TOC and 0.41 mg/g TOC while those for lacustrine shale are 66.92 mg/g TOC and 43.98 mg/g TOC, respectively. The results suggest that grain-based pyrolysis is more likely to reflect both generation and expulsion process. According to the above results, the expulsion/retention capability of two samples in this study can be evaluated. The lacustrine shale enjoys higher ability to retain hydrocarbon. The results are coincided with the observations in both field and laboratory. The grain-based Rock-Eval pyrolysis method presented in this study could be used to quickly evaluate the evolution of hydrocarbon generation, expulsion and retention.

Contributors

Lingling Liao completed the experiments, acquired data and drafted the paper. Yunpeng Wang designed experiments and finalized the manuscript. Chengsheng Chen and Shuyong Shi processed samples. Rui Deng plotted figures.

References

Abbassi, S., Edwards, D.S., George, S.C., Volk, H., Mahlstedt, N., di Primio, R., Horsfield, B., 2016. Petroleum potential and kinetic models for hydrocarbon generation from the upper cretaceous to paleogene latrobe group coals and shales in the gippsland basin, Australia. Org. Geochem. 91, 54–67.

Behar, F., Beaumont, V., Penteado, H.D.B., 2001. Rock-Eval 6 technology: performances and developments. Oil Gas Sci. Technol. 56, 111–134.

Behar, F., Kressmann, S., Rudkiewicz, J., Vandenbroucke, M., 1992. Experimental simulation in a confined system and kinetic modelling of kerogen and oil cracking. Org. Geochem. 19, 173–189.

Behar, F., Vandenbroucke, M., Tang, Y., Marquis, F., Espitalie, J., 1997. Thermal cracking of kerogen in open and closed systems: determination of kinetic parameters and stoichiometric coefficients for oil and gas generation. Org. Geochem. 26, 321–339.

Blanc, P., Connan, J., 1992. Generation and expulsion of hydrocarbons from a Paris Basin Toarcian source rock: An experimental study by confined-system pyrolysis. Energy & fuels 6, 666–677.

Braun, R.L., Burnham, A.K., 1990. Mathematical model of oil generation, degradation, and expulsion. Energy & Fuels 4, 132–146.

Burnham, A.K., Braun, R.L., 1999. Global kinetic analysis of complex materials. Energy & Fuels 13, 1–22.

Burnham, A.K., Braun, R.L., Gregg, H.R., Samoun, A.M., 1987. Comparison of methods for measuring kerogen pyrolysis rates and fitting kinetic parameters. Energy & Fuels 1, 452–458.

Cornford, C., Gardner, P., Burgess, C., 1998. Geochemical truths in large data sets. I: geochemical screening data. Org. Geochem. 29, 519–530.

Dai, J., Zou, C., Dong, D., Ni, Y., Wu, W., Gong, D., Wang, Y., Huang, S., Huang, J., Fang, C., 2016. Geochemical characteristics of marine and terrestrial shale gas in China. Mar. Petroleum Geol. 76, 444–463.

Dembicki, H., 1992. The effects of the mineral matrix on the determination of kinetic parameters using modified Rock Eval pyrolysis. Org. Geochem. 18, 531–539.

Espitalié, J., Laporte, J.L., Madec, M., Marquis, F., Leplat, P., Paulet, J., Boutefeu, A., 1977. Méthode rapide de caractérisation des roches mètres, de leur potentiel pétrolier et de leur degré d'évolution. Oil Gas Sci. Technol. 32, 23–42.

Gao, L., Schimmelmann, A., Tang, Y., Mastalerz, M., 2014. Isotope rollover in shale gas observed in laboratory pyrolysis experiments: Insight to the role of water in thermogenesis of mature gas. Org. Geochem. 68, 95–106.

Geng, A., Liao, Z., 2002. Kinetic studies of asphaltene pyrolyses and their geochemical applications. Appl. Geochem. 17, 1529–1541.

Han, S., Horsfield, B., Zhang, J., Chen, Q., Mahlstedt, N., di Primio, R., Xiao, G., 2014. Hydrocarbon generation kinetics of lacustrine Yanchang shale in southeast ordos basin, north China. Energy & Fuels 28, 5632–5639.

Inan, S., 2000. Gaseous hydrocarbons generated during pyrolysis of petroleum source rocks using unconventional grain-size: implications for natural gas composition. Org. Geochem. 31, 1409–1418.

İnan, S., Schenk, H.J., 2001. Evaluation of petroleum generation and expulsion from a source rock by open and restricted system pyrolysis experiments. Part I. extrapolation of experimentally-derived kinetic parameters to natural systems. J. Anal. Appl. Pyrolysis 58, 213–228.

Inan, S., Yalçin, M.N., Mann, U., 1998. Expulsion of oil from petroleum source rocks: inferences from pyrolysis of samples of unconventional grain size. Org. Geochem. 29, 45–61.

Jia, W., Wang, Q., Liu, J., Peng, P.a., Li, B., Lu, J., 2014. The effect of oil expulsion or retention on further thermal degradation of kerogen at the high maturity stage: A pyrolysis study of type II kerogen from Pingliang shale. China. Org. Geochem. 71, 17–29.

Langford, F., Blanc-Valleron, M.-M., 1990. Interpreting rock-Eval pyrolysis data using graphs of pyrolizable hydrocarbons vs. Total organic carbon (1). AAPG Bull. 74, 799–804.

Lehne, E., Dieckmann, V., 2007. The significance of kinetic parameters and structural markers in source rock asphaltenes, reservoir asphaltenes and related source rock kerogens, the Duvernay Formation (WCSB). Fuel 86, 887–901.

Liao, L., Wang, Y., Lu, J., 2016. Experimental study on fractional compositions of residual oil from shale and coal of China using grain-based MSSV pyrolysis. Energy & Fuels 30, 256–263.

Liu, X., Xiong, J., Liang, L., 2015. Investigation of pore structure and fractal characteristics of organic-rich Yanchang formation shale in central China by nitrogen adsorption/desorption analysis. J. Nat. Gas Sci. Eng. 22, 62–72.

Menzinger, M., Wolfgang, R., 1969. The meaning and use of the Arrhenius activation energy. Angewandte Chemie Int. Ed. Engl. 8, 438–444.

Miura, K., 1995. A new and simple method to estimate f (E) and k0 (E) in the distributed activation energy model from three sets of experimental data. Energy & Fuels 9, 302–307.

Pepper, A.S., Corvi, P.J., 1995. Simple kinetic models of petroleum formation. Part I: oil and gas generation from kerogen. Mar. Petroleum Geol. 12, 291–319.

Schenk, H., Di Primio, R., Horsfield, B., 1997. The conversion of oil into gas in petroleum reservoirs. Part 1: comparative kinetic investigation of gas generation from crude oils of lacustrine, marine and fluviodeltaic origin by programmed-temperature closed-system pyrolysis. Org. Geochem. 26, 467–481.

Schenk, H., Horsfield, B., 1993. Kinetics of petroleum generation by programmed-temperature closed-versus open-system pyrolysis. Geochimica Cosmochimica Acta 57, 623–630.

Sykes, R., Snowdon, L., 2002. Guidelines for assessing the petroleum potential of coaly source rocks using Rock-Eval pyrolysis. Org. Geochem. 33, 1441–1455.

Tang, Y., Perry, J., Jenden, P., Schoell, M., 2000. Mathematical modeling of stable carbon isotope ratios in natural gases. Geochimica Cosmochimica Acta 64, 2673–2687.

Tang, Y., Stauffer, M., 1994. Multiple cold trap pyrolysis gas chromatography: a new technique for modeling hydrocarbon generation. Org. Geochem. 22, 863–872.

Tissot, B., Espitalie, J., 1975. L'evolution thermique de la matière organique des sédiments: applications d'une simulation mathématique. Potentiel pétrolier des bassins sédimentaires de reconstitution de l'histoire thermique des sédiments. Oil Gas Sci. Technol. 30, 743–778.

Tissot, B., Pelet, R., Ungerer, P., 1987. Thermal history of sedimentary basins, maturation indices, and kinetics of oil and gas generation. AAPG Bull. 71, 1445–1466.

Tissot, B.P., Welte, D.H., 1984. Petroleum Formation and Occurrence.

Ungerer, P., 1990. State of the art of research in kinetic modelling of oil formation and expulsion. Org. Geochem. 16, 1–25.

Ungerer, P., Pelet, R., 1987. Extrapolation of the Kinetics of Oil and Gas Formation from Laboratory Experiments to Sedimentary Basins.

Wang, Y., Zhang, S., Wang, F., Wang, Z., Zhao, C., Wang, H., Liu, J., Lu, J., Geng, A., Liu, D., 2006. Thermal cracking history by laboratory kinetic simulation of Paleozoic oil in eastern Tarim Basin, NW China, implications for the occurrence of residual oil reservoirs. Org. Geochem. 37, 1803–1815.

Wei, Z., Zou, Y.-R., Cai, Y., Wang, L., Luo, X., Peng, P.a, 2012. Kinetics of oil group-type generation and expulsion: An integrated application to Dongying Depression, Bohai Bay Basin, China. Org. Geochem. 52, 1–12.

Xu, W., Guo, Y., Liu, J., Gao, J., Zhao, Z., 2013. Wulalike-Kelimoli Petroleum System of the West Margin of Ordos Basin, China, IPTC 2013: International Petroleum Technology Conference.

Zeng, L., Gao, C., Qi, J., Wang, Y., Li, L., Qu, X., 2008. The distribution rule and seepage effect of the fractures in the ultra-low permeability sandstone reservoir in east Gansu Province, Ordos Basin. Science in China Series D. Earth Sci. 51, 44–52.